Hindawi
Journal of Advanced Transportation
Volume 2020, Article ID 8136939, 6 pages
https://doi.org/10.1155/2020/8136939

Research Article

Wheel/Rail Adhesion State Identification of Heavy-Haul Locomotive Based on Particle Swarm Optimization and Kernel Extreme Learning Machine

Jianhua Liu,[1] **Linfan Liu**,[2] **Jing He**,[2] **Changfan Zhang**,[1] **and Kaihui Zhao**[2]

[1]*College of Traffic Engineering, Hunan University of Technology, Zhuzhou 412007, China*
[2]*College of Electrical and Information Engineering, Hunan University of Technology, Zhuzhou 412007, China*

Correspondence should be addressed to Jing He; hejing@263.net

Received 10 April 2019; Revised 22 July 2019; Accepted 14 August 2019; Published 10 January 2020

Academic Editor: Paola Pellegrini

The traction performance of heavy-haul locomotive is subject to the wheel/rail adhesion states. However, it is difficult to obtain these states due to complex adhesion mechanism and changeable operation environment. According to the influence of wheel/rail adhesion utilization on locomotive control action, the wheel/rail adhesion states are divided into four types, namely normal adhesion, fault indication, minor fault, and serious fault in this work. A wheel/rail adhesion state identification method based on particle swarm optimization (PSO) and kernel extreme learning machine (KELM) is proposed. To this end, a wheel/rail state identification model is constructed using KELM, and then the regularization coefficient and kernel parameter of KELM are optimized by using PSO to improve its accuracy. Finally, based on the actual data, the proposed method is compared with PSO support vector machines (PSO-SVM) and basic KELM, respectively, and the results are given to verify the effectiveness and feasibility of the proposed method.

1. Introduction

The traction performance of heavy-haul locomotive depends on the utilization efficiency of wheel/rail adhesion state [1–4], and the adhesion force required to operate locomotive is achieved by adjusting the creep velocity, which can be controlled by adjusting the output torque of traction motor. Different creep velocities show different wheel/rail adhesion states; a low creep velocity indicates that the wheel/rail adhesion performance is not fully utilized, while an extremely high creep velocity results in wheel/rail adhesion failure such as wheel/rail sliding. However, identifying wheel/rail adhesion states is difficult due to the complex operation environment and the subjectivity of manual adjustment. According to the influence of adhesion utilization on locomotive control action, the wheel/rail adhesion states are divided into four types, namely normal adhesion, fault indication, minor fault and serious fault [5]. Different wheel/rail adhesion states must be controlled using different methods. Effective identification of these sates can provide support for improving wheel/rail adhesion utilization performance.

The wheel/rail adhesion state of heavy-haul locomotive is a specific presentation of wheel to rail contact process, and it is decided by creep velocity and wheel/rail adhesion coefficient [6]. Domestic and foreign scholars have proposed some wheel/rail adhesion state identification methods, which have been summarized in a very recent review [7]. Simply, these methods can be classified as model-based methods and data-based identification methods.

The model-based methods created a relationship between locomotive operational parameters and wheel/rail adhesion state in the form of a mathematical model [8, 9]. The inputs of the models were directly measured data collected from sensors, and the outputs were the adhesion coefficients or other related measurable parameters such as slip/creep and acceleration [10, 11]. However, the main challenge of the model-based methods is to create a model that exactly characterizes the physical system in all conditions, and the identification of its precision is impacted by uncertain nonlinear parameters, unknown noises, and others factors. However, the main challenge of the model-based methods is to create a model that exactly characterizes the physical system under all conditions.

Also, the precision of identification is affected by uncertain nonlinear parameters, unknown noises and other factors.

In the data-based identification methods, the data-based model structure was pre-designed in advance, and the parameters of these model structures were optimized by using experimental data, and then, the trained models were used to identify wheel/rail adhesion states [12–15]. The family of the Kalman filter methods can minimise mean-squared estimation error for a linear stochastic system [17–20]. Artificial neural networks (ANNs), KELM, and other network-based methods use predetermined numbers of neurons that are connected to each other to accomplish defined actions [21, 22]. However, the parameters of data-based models were sensitive to noise, and the identification accuracy cannot be satisfied until the model parameters can be updated when environmental conditions change.

Also, the predefined model parameters were updated to improve the identification accuracy when environmental conditions change. A multiple models approach with variable parameters was proposed for friction estimation [23, 24], and a swarm intelligence algorithm was used to estimate adhesion condition. Compared with predefined models [23, 24] that were developed on the basis of the physical mechanism of wheel to rail, a data-based wheel/rail adhesion state identification model was presented by using KELM in our previous work [21], but the regularization coefficient and kernel parameter of this model must be manually adjusted according to the environment condition. Therefore, PSO is used to optimize the kernel parameter and regular coefficient of KELM, and the wheel/rail adhesion state identification model with variable parameters of KELM is developed to adapt the changing environment condition in this work.

This paper is structured as follows. The second section introduces the wheel/rail adhesion state identification strategy, the third section constructs the KELM-based identification model with optimal parameters, the fourth section presents the simulation and result analysis, and the fifth section is the conclusions.

2. Wheel/Rail Adhesion State Identification Model Strategy

2.1. Problem Analysis. Under the action of locomotive gravity, the contact component of wheel and rail produces elastic deformation. Meanwhile, the contact area becomes an approximate elliptical contact spot composed of creep and adhesion zones, as shown in Figure 1 [25, 26]. The wheel-to-rail contact in the creep zone produces a relative microscopic sliding phenomenon (namely creep), but the wheel and the rail are relatively stationary in the adhesion zone.

In Figure 1, v is the velocity of locomotive body; r is the rolling wheel radius; ω is the angular velocity of the wheel; P and P' are the vertical forces of the wheels and rails, respectively. When driving torque M acts on the locomotive wheel, it produces tangential force acting on wheel/rail contact surface F_T and tangential force acting on the contact surface of the rail F_T', thereby causing the wheel to roll forward. The velocity v is always less than the linear velocity of the wheel

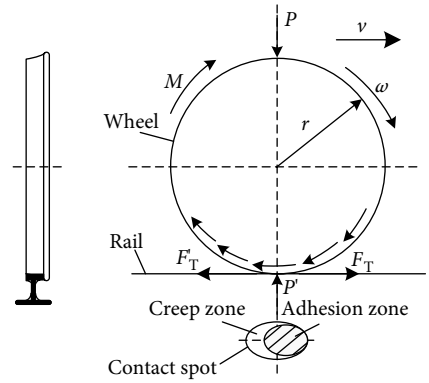

Figure 1: Wheel/rail adhesion-creep phenomenon.

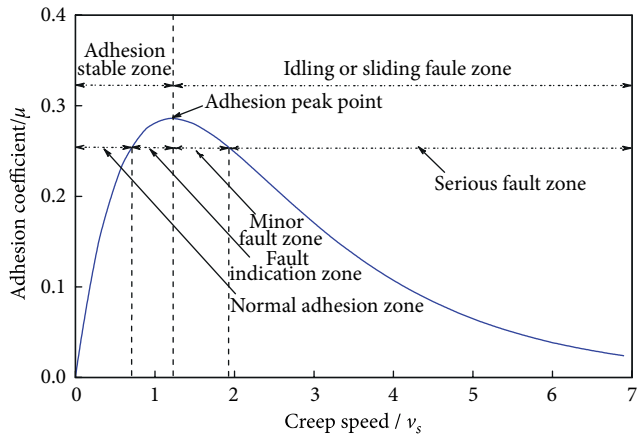

Figure 2: Wheel/rail adhesion-creep changing curve.

pair ωr because of the creep movement between the wheel and the rail in the creep zone. The difference in velocity between the two can be expressed as creep velocity v_s.

$$v_s = v - \omega r. \tag{1}$$

Wheel/rail adhesion coefficient μ is defined as the ratio of the maximum tangential force to the vertical force of the wheel to rail, which can be transmitted between F_T and P [25, 26].

$$\mu = \frac{F_T}{P}. \tag{2}$$

Wheel/rail adhesion is a very complicated process that is affected by many factors [27–29], including wheel/rail contact interface, locomotive velocity, and weather conditions. Although adhesion-creep characteristic curves vary under different working conditions [30], all adhesion-creep characteristic curves show similar change in trend characteristics; that is, each curve has an adhesion peak point, μ_{max}. The left area of the adhesion peak point is the adhesion stable zone, and the right area is the idling or sliding fault zone, as shown in Figure 2.

From Figure 2, the adhesion stable zone consists of normal adhesion zone and fault indication zone, whereas the idling or sliding fault zone consists of small fault zone and serious fault zone. In the normal adhesion zone, the adhesion

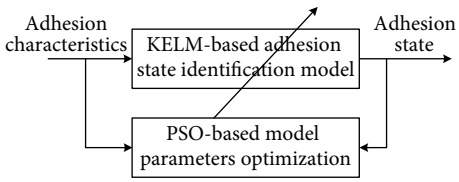

Figure 3: Framework of establishing wheel/rail adhesion state identification model based on KELM and PSO.

coefficient and creep velocity have an approximate linear relation when train driving force is small. In the fault indication zone located in a small field on the left side of the adhesion peak point, if the traction increases further at this zone, the adhesion state will fall into idling or sliding fault zone located on the right side of the adhesion peak point. In the minor fault zone, the adhesion coefficient decreases sharply with the increase in creep velocity; meanwhile, small sliding occurs between the wheel and the rail. In the serious fault zone, the wheel pair exhibits an evident idling or sliding phenomenon, and the wheels and rails produce severe wear that affects the safety of operation in serious cases. The adhesion state of different zones must be controlled using different methods. For instance, the torque output should be increased to improve the adhesion utilization rate when the adhesion coefficient is located in the normal adhesion zone, but it also should be fine-tuned to avoid the occurrence of fault when the adhesion coefficient is located in the fault indication zone. Meanwhile, the torque output should be reduced to convert the adhesion coefficient into the adhesion stable zone when the adhesion coefficient is located in the small fault zone, and it should be greatly reduced to ensure safety when the adhesion coefficient is located in the serious fault zone. Therefore, effective identification of wheel/rail adhesion state of different zones is required to provide support for the purposeful implementation of adhesion control.

2.2. Model Framework. In fact, the characteristics of wheel/rail adhesion change with the varying of rail surface state. For example, the wheel/rail adhesion coefficient on the ice/snow or greasy surface is much smaller than that on the dry rail surface. Hence, the wheel/rail adhesion state identification model is difficult to establish with fixed parameters; instead, it should be analyzed by using the real-time operational data. Therefore, a KELM-based wheel/rail adhesion identification model has been proposed by the authors of this paper [21], but the model parameters must be adjusted manually according to various environments. Based on our previous research work [21], a novel KELM-based wheel/rail adhesion identification model is proposed in this work, and PSO is used to optimize the model parameters, as shown in Figure 3.

Based on the model framework and the problem analysis above, wheel/rail adhesion coefficient and creep velocity are selected as the inputs of identification model, and the model outputs are the four wheel/rail adhesion states including normal adhesion, fault indication, minor fault, and serious fault. By using the historical date, the wheel/rail adhesion state identification model based on KELM is proposed, and the PSO algorithm is used to optimize the regular coefficient and kernel parameter of KELM in order to improve identification performance.

3. Wheel/Rail Adhesion State Identification Model

3.1. Kernel Extreme Learning Machine (KELM). KELM is an improved algorithm combing extreme learning machine (ELM) with kernel function [31], where ELM is a single implicit layer feed-forward neural network (SLFN) [32, 33]. The advantage of ELM lies in its easy implementation, fast learning, and generalization ability [34]. Given N training data $D = \{(x_i, y_i), i = 1, 2, \ldots, N\}$, where, x_i is the i^{th} input data, y_i is the i^{th} output value, the SLFNs with L hidden layer nodes can be expressed as [32, 33]

$$\hat{y}(x) = f(x) = h(x) \cdot \beta = H \cdot \beta, \tag{3}$$

where, $\hat{y}(x) = f(x)$ is the output of SLFNs; $h(x) = H$ is the kernel mapping matrix of the hidden layer; β is the weight between hidden layer and output layer. ELM trains the network with minimal training error and minimal output weight norm, and the trained weight can be expressed as [34]

$$\beta = H^{\mathrm{T}}\left(\frac{I}{C} + HH^{\mathrm{T}}\right)^{-1} y, \tag{4}$$

where, I is a unit matrix; y is the output vector matrix, $y = [y_1, y_2, \ldots, y_N]$; C is a regularization coefficient that is used to deviate the eigenvalue of HH^{T} from zero.

Formula (4) is substituted into Formula (3), and the ELM is obtained

$$\hat{y}(x) = f(x) = h(x)H^{\mathrm{T}}\left(\frac{I}{C} + HH^{\mathrm{T}}\right)^{-1} y. \tag{5}$$

Based on Mercer's condition, the kernel matrix is defined as [35],

$$\begin{aligned} \Omega_{\mathrm{ELM}} &= HH^{\mathrm{T}} \\ \Omega_{i,j} &= h(x_i) \cdot h(x_j) = K(x_i, x_j). \end{aligned} \tag{6}$$

Using Formulas (5) and (6), the ELM-based identification model can be expressed as

$$\hat{y}(x) = f(x) = \begin{bmatrix} K(x, x_1) \\ \vdots \\ K(x, x_N) \end{bmatrix}^{\mathrm{T}} \left(\frac{I}{C} + \Omega_{\mathrm{ELM}}\right)^{-1} y. \tag{7}$$

Many types of kernel functions, such as linear, polynomial, Gaussian radial, and sigmoid, are available. Among these types, Gaussian radial basis function (RBF) is widely used, and its formula can be expressed as

$$K(x, x_i) = \exp\left(-\frac{\|x - x_i\|^2}{\delta^2}\right), \tag{8}$$

where, δ is the kernel parameter.

3.2. PSO-Based Model Parameters Optimization. The regularization coefficient C in Formula (5), and the kernel parameters δ in Formula (8) are generally set according to artificial experience. However, such setting often leads to the unreliable identification accuracy due to the blindness. Moreover, the two parameters must be updated in real time if the operation environment changes, thereby limiting its practical application in the system. In this work, based on historical data, the model parameters are updated by using PSO algorithm, and acceptable identification accuracy is obtained.

Let $X_i = (x_{i1}, x_{i2}, \ldots, x_{in})$ denote the particle position vector and $V_i = (v_{i1}, v_{i2}, \ldots, v_{in})$ denote the particle velocity vector; then, the velocity and position of PSO update formula that can be respectively expressed as [36]

$$v_{id}^{k+1} = \omega v_{id}^{k} + c_1 r_1 \left(p_{id}^{k} - x_{id}^{k}\right) + c_2 r_2 \left(p_{gd}^{k} - x_{id}^{k}\right), \quad (9)$$

$$x_{id}^{k+1} = x_{id}^{k} + v_{id}^{k+1}, \quad (10)$$

where, ω is the inertial weight, k is the current iteration number, p_{id}^{k} is the individual optimal particle position, P_{gd}^{k} is the global optimal particle position, c_1 and c_2 represent the acceleration coefficients, r_1 and r_2 are the random numbers distributed between [0, 1].

The inertial weight ω is updated by

$$\omega = \omega_{\max} - \frac{t\left(\omega_{\max} - \omega_{\min}\right)}{t_{\max}}, \quad (11)$$

where, t and $t_{\max}$ denote the current iteration number and maximum iteration number, respectively.

The details of the PSO algorithm have been discussed in [37].

3.3. Detailed Algorithm. Based on the analysis above, select wheel/rail adhesion coefficient and creep velocity as the inputs of wheel/rail adhesion state identification model, and the model outputs are normal adhesion, fault indication, minor fault, and serious fault. The flow chart of wheel/rail adhesion state identification model proposed here is depicted in Figure 4.

The detailed steps of the wheel/rail adhesion state identification model are as follows:

Step 1: Dividing the data sample set into the training sample set and testing sample set, and normalizing them.

Step 2: Setting the value range of regularization coefficient C in Formula (5) and the kernel parameters δ in Formula (8), and initializing the parameters of PSO.

Step 3: Training the model parameters using Formula (7).

Step 4: Calculating the fitness value of the testing sample by taking the model identification accuracy as the fitness function.

Step 5: Updating the velocity vector, position vector, and inertial weight by using Formulas (9)–(11).

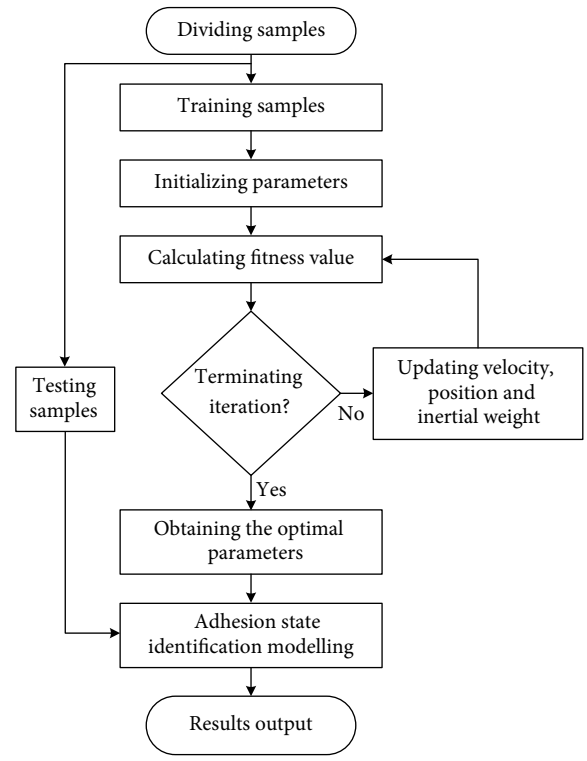

Figure 4: Flow chart of adhesion state identification model based on KELM and PSO.

Step 6: Terminating the iteration process if the fitness value meets the pre-set condition or if the number of iterations reaches the set value, and the optimized regularization coefficient and the kernel parameter are obtained. Otherwise, return to Step 4.

Step 7: Updating the regularization coefficient and the kernel parameter in Formula (7), the novel wheel/rail adhesion state identification model is obtained.

In addition, as the sample data are continuously updated, the optimal regularisation coefficient and the kernel parameter can be obtained according the above steps.

4. Results and Discussion

In this work, the data were collected from RT-LAB Test Stand that includes mechanical sub-model and traction transmission sub-model of heavy-haul locomotive. The mechanical sub-model was developed with ADAMS/Rail in our previous work [38, 39], while the traction transmission sub-model was also established using MATLAB/Simulink in our previous work [6], and then, the traction transmission sub-model was placed into RT-LAB Test Stand, with the same parameters as that of HXD1 heavy haul locomotive [6]. The data with different types of wheel/rail adhesion states were obtained by adjusting the torque output of motor, and they are collected from the wheelset of a single motor drive. The 3,000 data collected are encoded as four types (normal adhesion, fault indication, small fault and serious fault) according to the velocity

Table 1: The comparison table of testing results of three methods.

Method	Running time (s)	Identification accuracy (%)
PSO-SVM	33.85	85.11
KELM	0.49	87.00
Proposed method (PSO-KELM)	18.68	92.60

difference between wheel and roller. Each type of data is divided into training and testing sample sets following a 2 : 1 ratio. Data simulation is performed on a computer with a Core i3-4170 processor and 16 GB memory, and the simulation platform is MATLAB 2010a.

In order to test the performance of the proposed method, the PSO-SVM and basic KELM are chosen as the comparison methods, and the training samples and testing samples of each algorithm are the same. The regularisation coefficient and the kernel parameter of the proposed method are optimized by PSO, but the parameters of other methods are manually set by multiple trials. Particularly, the kernel parameter of basic KELM is $\delta = 17.2$, and the regularization coefficient C and the kernel parameter δ of PSO-SVM are 1/16.1 and 101, respectively. In addition, the PSO-SVM is implemented with the LIBSVM tool developed by Professor Lin [40]. The testing results are shown in Table 1.

Table 1 shows that the running time with training samples of PSO-SVM method and the proposed PSO-KELM method is greater than that of KELM method, that is because the PSO-SVM method needs to optimize the classification hyperplane and the proposed PSO-KELM method needs to optimize the regularization coefficient and kernel parameters. In fact, when using the testing samples to test the performance of the proposed method, the running time is very little that can be ignored as the model has been developed. The identification accuracy with PSO-SVM, KELM, and the proposed method is 85.11%, 87.00% and 92.60%, respectively. Compared with PSO-SVM method and KELM, the results of adhesion state identification obtained using the proposed method are 8.8% and 6.44% higher, respectively. Therefore, the proposed algorithm can potentially be used as a wheel/rail adhesion state identification tool for locomotive.

Additionally, though our work focuses on the heavy-haul locomotive, we think that the proposed method also applies to the train, given the same wheel/rail mechanism. Related experimental verification is our next research focus.

5. Conclusions

Effective wheel-rail adhesion state identification is the basis of adhesion control for heavy-haul locomotive. A method to identify the wheel/rail adhesion state of heavy-haul locomotive is developed by using PSO and KELM in this work. The kernel function is introduced into the KELM to avoid the output fluctuation and blind problem of the hidden layer node setting caused by the random matrix selection in traditional extreme learning. The model parameters of KELM are optimized in real time by using PSO to improve the environmental adaptability of the identification model. The results of experimental comparison and analysis indicate that the proposed method is better than PSO-SVM and KELM.

Data Availability

The data used to support the findings of this study are available from the corresponding author upon request.

Disclosure

The statements made herein are solely the responsibility of the authors.

Conflicts of Interest

The authors declare that they have no conflicts of interest.

Acknowledgments

This work was supported by the Natural Science Foundation of China [grant number 61773159] and Excellent Youth Research Project of Education Department of Hunan Province [18B303], and Hunan Provincial Natural Science Foundation of China [grant numbers 2018JJ2100 and 2018JJ2093].

References

[1] M. Spiryagin, P. Wolfs, F. Szanto, and C. Cole, "Simplified and advanced modelling of traction control systems of heavy-haul locomotives," *Vehicle System Dynamics*, vol. 53, no. 5, pp. 672–691, 2015.

[2] L. B. Shi, L. Ma, J. Guo, Q. Y. Liu, Z. R. Zhou, and W. J. Wang, "Influence of low temperature environment on the adhesion characteristics of wheel-rail contact," *Tribology International*, vol. 127, pp. 59–68, 2018.

[3] L. Zhang and X. Zhuan, "Optimal operation of heavy-haul trains equipped with electronically controlled pneumatic brake systems using model predictive control methodology," *IEEE Transactions on Control Systems Technology*, vol. 22, no. 1, pp. 13–22, 2013.

[4] W. R. Liu, D. Y. Wang, K. Gao, and Z. W. Huang, "Design of distributed cooperative observer for heavy-haul train with unknown displacement," *IET Intelligent Transport Systems*, vol. 11, no. 4, pp. 239–247, 2017.

[5] J. He, L. F. Liu, C. F. Zhang, K. H. Zhao, J. Sun, and P. Li, "Deep denoising autoencoding method for feature extraction and recognition of vehicle adhesion status," *Journal of Sensors*, vol. 2018, Article ID 5419645, 8 pages, 2018.

[6] C. F. Zhang, J. Sun, J. He, and L. F. Liu, "Online estimation of the adhesion coefficient and its derivative based on the cascading SMC observer," *Journal of Sensors*, vol. 2017, Article ID 8419295, 11 pages, 2017.

[7] S. Shrestha, Q. Wu, and M. Spiryagin, "Review of adhesion estimation approaches for rail vehicles," *International Journal of Rail Transportation*, vol. 7, no. 2, pp. 79–102, 2019.

[8] F. W. Carter, "On the action of a locomotive driving wheel," *Proceedings of the Royal Society A: Mathematical, Physical and Engineering Sciences*, vol. 112, no. 760, pp. 151–157, 1926.

[9] C. P. Ward, R. M. Goodall, R. Dixon, and G. A. Charles, "Adhesion estimation at the wheel-rail interface using advance model-based filtering," *Vehicle System Dynamics*, vol. 50, no. 12, pp. 1797–1816, 2012.

[10] I. Hussain, T. X. Mei, and R. T. Ritchings, "Estimation of wheel-rail contact conditions and adhesion using the multiple model approach," *Vehicle System Dynamics*, vol. 51, no. 1, pp. 32–53, 2013.

[11] T. Zhu, S. Xiao, G. Yang, W. Ma, and Z. Zhang, "An inverse dynamics method for railway vehicle systems," *Transport*, vol. 29, no. 1, pp. 107–114, 2014.

[12] J. J. Castillo, J. A. Cabrera, A. J. Guerra, and A. Simon, "A novel electrohydraulic brake system with tire–road friction estimation and continuous brake pressure control," *IEEE Transactions on Industrial Electronics*, vol. 63, no. 3, pp. 1863–1875, 2016.

[13] W. C. Cai, W. Liao, D. Li, and Y. Song, "Observer based traction/braking control design for high speed trains considering adhesion nonlinearity," *Abstract and Applied Analysis*, vol. 2014, Article ID 968017, 10 pages, 2014.

[14] W. C. Cai, D. Li, and Y. Song, "A novel approach for active adhesion control of high-speed trains under antiskid constraints," *IEEE Transactions on Intelligent Transportation Systems*, vol. 16, no. 6, pp. 3213–3222, 2015.

[15] G. Xu, K. Xu, C. Zheng, and T. Zahid, "Optimal operation point detection based on force transmitting behavior for wheel slip prevention of electric vehicles," *IEEE Transactions on Intelligent Transportation Systems*, vol. 17, no. 2, pp. 481–490, 2016.

[16] P. Pichlík and J. Zděnek, "Adhesion force detection method based on the Kalman filter for slip control purpose," *Automatika*, vol. 57, no. 2, pp. 405–415, 2016.

[17] I. Hussain, T. X. Mei, and M. Mirzapour, "Real time estimation of the wheel-rail contact conditions using multi-Kalman filtering and fuzzy logic," in *Proceedings of 2012 UKACC International Conference on Control*, IEEE, Cardiff, UK, 2012.

[18] P. D. Hubbard, C. Ward, R. Dixon, and R. Goodall, "Models for estimation of creep forces in the wheel/rail contact under varying adhesion levels," *Vehicle System Dynamics*, vol. 51, no. 1, pp. 370–386, 2014.

[19] P. D. Hubbard, C. Ward, R. Dixon, and R. Goodall, "Verification of model-based adhesion estimation in the wheel-rail interface," *Chemical Engineering Transactions*, vol. 33, pp. 757–762, 2013.

[20] S. Strano and M. Terzo, "On the real-time estimation of the wheel-rail contact force by means of a new nonlinear estimator design model," *Mechanical Systems and Signal Processing*, vol. 105, pp. 391–403, 2018.

[21] C. F. Zhang, X. Cheng, J. He, and G. W. Liu, "Automatic recognition of adhesion states using an extreme learning machine," *International Journal of Robotics and Automation*, vol. 32, no. 2, pp. 194–200, 2017.

[22] S. Falomi, M. Malvezzi, E. Meli, and A. Rindi, "Determination of wheel-rail contact points: comparison between classical and neural network based procedures," *Meccanica*, vol. 33, no. 6, pp. 661–686, 2009.

[23] A. Onat and P. Voltr, "Velocity measurement-based friction estimation for railway vehicles running on adhesion limit: swarm intelligence-based multiple models approach," *Journal of Intelligent Transportation Systems*, vol. 23, pp. 1–15, 2019.

[24] A. Onat and P. Voltr, "Swarm intelligence based multiple model approach for friction estimation at wheel-rail interface," in *Proceedings of the 5th International Symposium on Engineering, Artificial Intelligence and Applications, ISEAIA 2017*, Cyprus, 2017.

[25] J. He, G. W. Liu, J. H. Liu, C. F. Zhang, and X. Cheng, "Identification of a nonlinear wheel/rail adhesion model for heavy-duty locomotives," *IEEE Access*, vol. 6, pp. 50424–50432, 2018.

[26] J. He, J. H. Liu, and C. F. Zhang, "An overview on wheel-rail adhesion utilization of heavy-haul locomotive (in Chinese)," *Journal of the China Railway Society*, vol. 40, no. 9, pp. 30–39, 2018.

[27] P. Voltr and M. Lata, "Transient wheel-rail adhesion characteristics under the cleaning effect of sliding," *Vehicle System Dynamics*, vol. 53, no. 5, pp. 605–618, 2015.

[28] G. Trummer, L. E. Buckley-Johnstone, P. Voltr, A. Meierhofer, R. Lewis, and K. Six, "Wheel-rail creep force model for predicting water induced low adhesion phenonmena," *Tribology International*, vol. 109, pp. 409–415, 2017.

[29] A. Onat, P. Voltr, and M. Lata, "A new friction condition identification approach for wheel-rail interface," *International Journal of Rail Transportation*, vol. 5, no. 3, pp. 127–144, 2017.

[30] T. Peng, Z. W. Guan, R. H. Zhang, J. S. Dong, K. N. Li, and H. G. Xu, "Bifurcation of lane change and control on highway for tractor-semitrailer under rainy weather," *Journal of Advanced Transportation*, vol. 2017, Article ID 3506053, 19 pages, 2017.

[31] G. B. Huang, "An insight into extreme learning machines: random neurons, random features and kernels," *Cognitive Computation*, vol. 6, no. 3, pp. 376–390, 2014.

[32] G. B. Huang, Q. Y. Zhu, and C. K. Siew, "Extreme learning machine: theory and applications," *Neurocomputing*, vol. 70, no. 13, pp. 489–501, 2006.

[33] G. B. Huang, H. X. Zhou, X. J. Ding, and R. Zhang, "Extreme learning machine for regression and multiclass classification," *IEEE Transactions on Systems, Man, and Cybernetics Part B (Cybernetics)*, vol. 42, no. 2, pp. 513–529, 2012.

[34] G. B. Huang, D. H. Wang, and Y. Lan, "Extreme learning machines: a survey," *International Journal of Machine Learning and Cybernetics*, vol. 2, no. 2, pp. 107–122, 2011.

[35] Z. Y. Huang, Y. L. Yu, J. Gu, and H. Liu, "An efficient method for traffic sign recognition based on extreme learning machine," *IEEE Transactions on Cybernetics*, vol. 47, no. 4, pp. 920–933, 2017.

[36] Y. Delice, E. K. Aydoğan, U. Özcan, and M. S. İlkay, "A modified particle swarm optimization algorithm to mixed-model two-sided assembly line balancing," *Journal of Intelligent Manufacturing*, vol. 28, no. 1, pp. 23–36, 2017.

[37] R. Thangaraj, M. Pant, A. Abraham, and P. Bouvry, "Particle swarm optimization: hybridization perspectives and experimental illustrations," *Applied Mathematics and Computation*, vol. 217, no. 12, pp. 5208–5226, 2011.

[38] J. He, B. B. Dou, C. F. Zhang, L. F. Liu, and X. F. Yin, "Anti-slip strategy of locomotives using improved adhesion characteristic curve slope method," in *Proceeding of the 2017 Chinese Automation Congress, CAC2007*, Jinan, China, 2017.

[39] C. F. Zhang, B. B. Dou, J. He, L. F. Liu, and X. F. Yin, "Study on locomotive anti-slip simulation based on axle load transfer," *Electric Drive for Locomotives*, vol. 2, pp. 35–38, 2017, (in Chinese).

[40] C. Chang and C. Lin, "LIBSVM: a library for support vector machine," *ACM Transactions on Intelligent Systems and Technology*, vol. 2, no. 3, pp. 1–39, 2014.